Age of Initiation of the India-Asia Collision in the East-Central Himalaya

Bin Zhu, William S. F. Kidd, David B. Rowley,[1] Brian S. Currie,[2] and Naseer Shafique[2]

Department of Earth and Atmospheric Sciences, University at Albany, Albany, New York 12222, U.S.A.
(e-mail: bz7463@csc.albany.edu)

ABSTRACT

We document the stratigraphy and provenance of the lower Tertiary terrigenous sections in the Zhepure Shan region of the Tethyan Himalaya, southern Tibet, using petrographic and geochemical whole-rock and single-grain techniques. The Cretaceous–early Tertiary shelf deposits of shallow marine carbonates and siliciclastics of the former Indian passive margin near the western end of the Zhepure Shan are conformably overlain by lower Tertiary clastic rocks. Sandstones in the Jidula Formation (Paleocene) mostly contain monocrystalline quartz grains of cratonic origin. In contrast, significant amounts of immature framework grains with a distinct ophiolitic and volcanic arc influence are present in the Youxia (Early Eocene) and Shenkeza (post–Early Eocene) formations. Major, trace, and rare earth element concentrations in both sandstones and shales complement the petrographic data and indicate that the source of the Jidula Formation consisted primarily of quartzose basement rocks, probably of Indian continental origin, whereas the sediments of the Youxia Formation were mainly derived from the uplifted Gangdese arc-trench system associated with the obduction of the Asian subduction complex. The compositions of Cr-rich spinels in the Youxia and Shenkeza sandstones resemble those from fore-arc peridotites and were most likely derived from the arc and ophiolite rocks along the developing Yarlung-Zangbo suture to the north. No spinels have been observed in the Jidula sandstones. Therefore, the early Tertiary detrital clastics in the Zhepure Shan record a marked change in provenance and sediment character and specifically at the time of deposition of the Youxia Formation, which contains a zone P-8 foram assemblage. This change indicates that the onset of India-Asia collision and the first development of the foreland basin immediately south of the India-Asia suture zone occurred at 50.6 ± 0.2 Ma in the both the western (Zanskar) and eastern (this study) Tethyan Himalaya.

Online enhancements: appendix tables.

Introduction

The age of initiation of the India-Asia collision remains a matter of considerable debate, with views ranging from Late Cretaceous (>65 Ma) to as young as 37 Ma (Rowley 1996, 1998, and references therein; de Sigoyer et al. 2000, 2001; Najman and Garzanti 2000; Yin and Harrison 2000; Searle 2001; Najman et al. 2002). The precise timing of the start of collision between India and Asia is significant for estimating mass balance in the Himalayan system because of the high rate of India-Asia motion during the 65–47 Ma interval (Patriat and Achache 1984; Le Pichon et al. 1992; Rowley 1996) and for

determining whether other events, including (1) changes in the India-Asia convergence rate between chrons 21 and 20 (Patriat and Achache 1984), (2) changes in India-Africa and India-Antarctica spreading directions between chrons 18 and 20, and (3) changes in ocean chemistry, most notably Sr isotopes at about 42 Ma (Richter et al. 1992), are potentially linked with the onset of this collision.

Sediment provenance in a foreland basin provides information on the tectonic evolution of the associated orogenic zone (Dickinson and Suczek 1979; Zuffa 1980; Ingersoll et al. 1984; Dickinson 1985; Garzanti et al. 1996; Clingolani et al. 2003), and it can constrain the age of the onset of collision (Rowley and Kidd 1981). For example, detailed stratigraphic and petrographical analysis of the Cretaceous to Eocene Tethyan sedimentary succession

in the Zanskar region, NW Himalaya (Garzanti et al. 1987, 1996), indicates that the India-Asia collision started there in the late Ypresian (~50.6 Ma). In this article, we report new data on the stratigraphy, sandstone petrology, geochemical composition, and spinel characteristics preserved in the lower Tertiary clastics exposed in the Zhepure Shan in the east-central Tethyan Himalaya of southern Tibet.

Geological Framework

The Tethyan Himalaya, located between the High Himalayan Crystalline belt to the south and the Indus-Yarlung-Zangbo Suture and the Lhasa block to the north (fig. 1), consist primarily of Late Paleozoic to Eocene marine sedimentary rocks, originally deposited along the northern passive continental margin of the Indian continent (Gansser 1964; Burg and Chen 1984). Deposition began with Late Paleozoic–Triassic rifting (Sengor et al. 1988; Sciunnach and Garzanti 1996; Garzanti 1999) during the initial development of the Neo-Tethyan Ocean, and a wide passive continental margin subsequently developed (Willems et al. 1996). During the mid-Cretaceous, northward-directed subduction of the Neo-Tethyan oceanic crust beneath the southern margin of Asia resulted in the development of the Gangdise magmatic arc and Xigaze fore-arc basin along the southern margin of the Lhasa block (Einsele et al. 1994; Durr 1996).

The India-Asia collision has been argued to have begun sometime in the Late Cretaceous–early Tertiary interval, with the Indus-Yarlung-Zangbo suture marking the site of removal of Neo-Tethys oceanic lithosphere. The strata of the Tethyan Himalaya record the development and subsequent closure of the Neo-Tethys and collision of India and Asia (Garzanti et al. 1987, 1996; Pivnik and Wells 1996; Rowley 1996; Najman et al. 1997, 2001; Najman and Garzanti 2000; Qayyum et al. 2001; Wan et al. 2002; Wang et al. 2002).

Lithostratigraphy in the Zhepure Shan Region

This study concentrates on the well-exposed Tertiary clastic rocks resting conformably above shallow marine carbonates and siliciclastics near the western end of the Zhepure Shan (fig. 2). The Zhepure Shan belongs to the southern continental shelf–dominated zone of the Tethyan Himalaya. The Cretaceous to early Tertiary sequence of the southern Tethyan Himalayan zone is best exposed in the ranges east of Gamba (Khampa Dzong) and west of Shekar Dzong (or New Tingri), regarded as
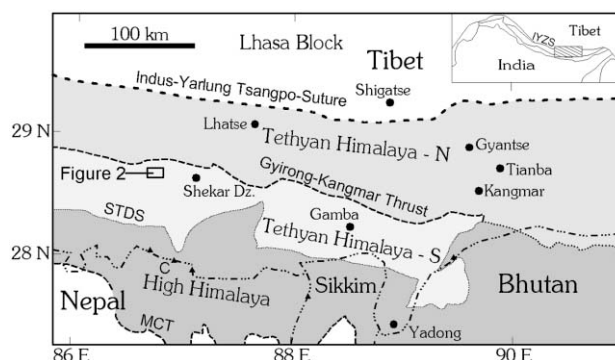
Figure 1. Simplified tectonic map of the east-central Tethyan Himalaya (modified after Willems et al. 1996). The inset map shows the position of this area in the Himalayan system. *MCT* = Main Central Thrust; *STDS* = Southern Tibet Detachment system; *C* = Cholmolungma.

local stratotypes for the Cretaceous and lower Tertiary in southern Tibet (Zhang and Geng 1983; Willems et al. 1996). Six stratigraphic units (fig. 3) have been defined in the Gongza section on the north slope of the Zhepure Shan mountain west of Shekar Dzong (Willems et al. 1996), with ages at the top of the section modified on the basis of work reported here. They are, from oldest to youngest, the Gamba Group (late Albian–early Santonian), consisting of marls and subordinate limestones; the Zhepure Shanbei Formation (early Santonian–middle Maastrichtian), comprising well-bedded limestones interbedded with very thin layers of marl; the Zhepure Shanpo Formation (middle Maastrichtian–Early Paleocene), consisting of a lower interval dominated by siliciclastic sandstones with minor calcareous sandstones and an upper sequence composed of pale-weathering, gray and black marlstone; the Jidula Formation (Danian) characterized by calcareous and glauconitic sandstones, shales, and mudstones; the Zhepure Shan Formation (late Danian–Ypresian), consisting of thick-bedded to massive limestones characterized by abundant large foraminifera; and the uppermost unit referred to by Willems et al. (1996) as the "Zongpubei Formation" (Ypresian or younger) of greenish-gray shales and some sandstones overlain by red clay and siltstone with intercalations of sandstones (Wang et al. 2002). The Gamba Group through Zhepure Shan Formation all represent shelf facies deposits of the Neo-Tethys and, in the Zhepure Shan region, contain a relatively continuous depositional record from Albian through the Ypresian. On the basis of the work of Willems et
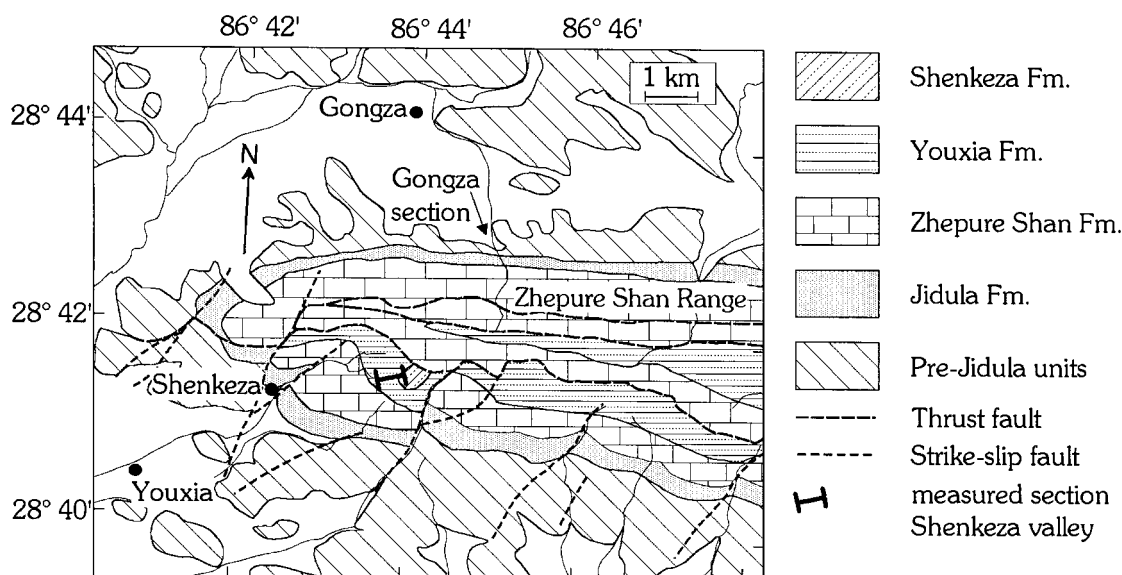
Figure 2. Simplified geologic map showing the location of the studied sections on the western end of the Zhepure Shan range. Interpretation extended from outcrop observations using Landsat TM image.

al. (1996), the Zhepure Shan limestones are the youngest well-dated marine sediments reported from the Tethyan Himalayas.

Siliciclastic sediments, stratigraphically the highest unit in the Zhepure Shan, were referred to as the Zongpubei Formation by Willems et al. (1996). These were thought to be correlative with siliciclastic sediments at the top of the Zhepure Shan Formation in the Gamba region (180 km to the ESE; fig. 1), named the Zongpubei Formation by Willems et al. (1996). There are several reasons for questioning this correlation. The sandstones in the Zongpubei at Gamba are distinctly different from the sandstones at the top of the section in the Zhepure Shan range near Tingri: sandstones in the Zongpubei Formation at Gamba are relatively quartz-rich, lithic-poor arenites, and no chrome spinel grains have been observed in the heavy mineral separates of a sandstone sample from this section. Second, in Gamba, the Zongpubei rests conformably at the top of the limestones of the Zhepure Shan Formation that are there dated only as young as Late Paleocene (Thanetian), whereas in the Zhepure Shan range near Tingri the limestones and overlying marine shales extend into the late Ypresian. Thus the two sequences are neither temporally correlative nor do they share similar provenance. For these reasons, we choose to refer to the siliciclastics in the Zhepure Shan as the Youxia Formation.

The Eocene clastics ("Zongpubei Formation") in

the Zhepure Shan region were not studied in detail by Willems et al. (1996) because of poor exposure and a fault contact between the unit and the underlying Zhepure Shan Formation in the section they examined. A better-exposed 180-m-thick section termed the "Pengqu Formation" was described by Wang et al. (2002); they reported the location as 5 km east of the Gongza section of Willems and Zhang (1993) and Willems et al. (1996). Wang et al. (2002) divided this section into the Enba Member consisting of gray and yellowish-green shale intercalated with sandstones and overlying red shale and sandstones that they named the Zhaguo Member; they described these strata as conformably overlying the massive limestones of the Zhepure Shan Formation.

During field studies in the Zhepure Shan region in October 2000, we also studied this section, which is actually located (fig. 2) only 2.5 km away from and southwest of the Gongza section in the head of the Shenkeza valley (86°43′39″E, 28°41′26″N). Although we observed a similar lithostratigraphic sequence consisting of green shales and thin-bedded sandstones in the lower part and red mudstones and sandstones in the upper part, we recognize a significant erosion surface and weathering profile (disconformity) between the green and red units. We therefore reject the proposal of Wang et al. (2002) that they should be included in a single formation.

For these Eocene clastic sediments exposed in the

Gongza Section
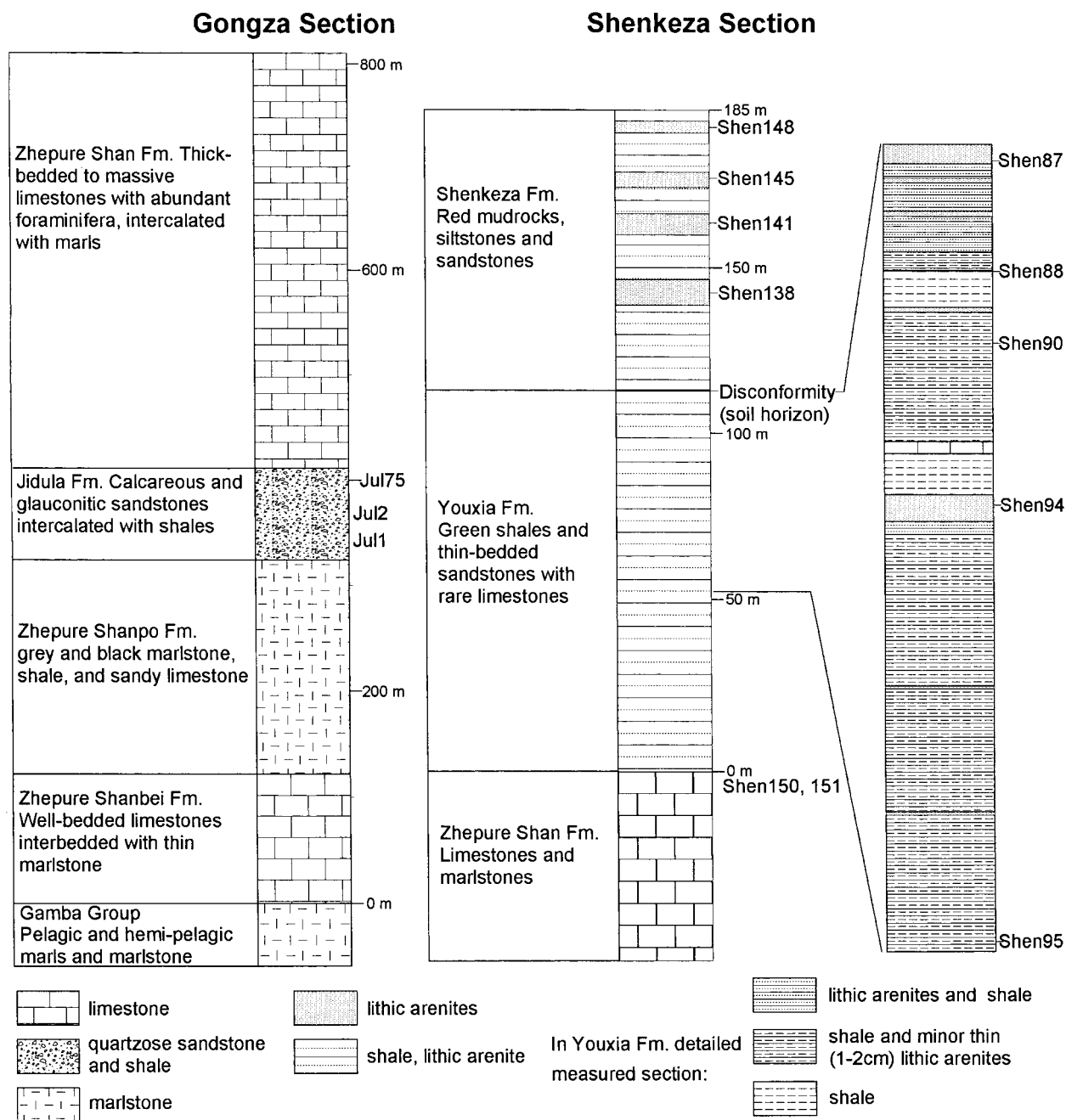
Shenkeza Section

Figure 3. Stratigraphic columns of lower Tertiary sequence in the Tingri region. The Shenkeza section was measured by us in 2000; the Gongza section is from Willems et al. (1996). Section locations are shown in figure 2. Sample positions are indicated by "Shen" plus a number in the Shenkeza section and "Jul" plus a number in the Gongza section.

head of the Shenkeza valley, we propose the name of Youxia Formation (named after a nearby village; fig. 2) for the 105-m-thick green shales and thin-bedded sandstones. On the basis of structural and lithological interpretation of the Landsat 7 ETM+ image, the extrapolation from the field observations indicates that the green clastic unit is widely distributed, although not commonly well exposed, along the center of the Zhepure mountain range. The unit can be identified on the basis of the struc-

Table 1. Planktonic Foraminifera Identified in Shen 90 from the Youxia Formation

Species	Abundance	Biostratigraphic range
Morozovella aragonensis	Common	P-8 to P-10
Morozovella lensiformis	Very rare	P-6 to P-8
Morozovella quetra	Very rare	P-5 to P-8
Morozovella aequa	Very rare	P-5 to P-8
Morozovella formosa gracilis	Rare	P-6 to P-8
Subbotina inaequispira	Common	Late Paleocene–Early Eocene
Globigernitheka cf. *higginis*	Rare	Late Early Eocene–Middle Eocene
Muricoglobigerina senni	Rare	Early–Middle Eocene
Chiloguembelina sp.	Rare	Paleocene–Eocene
Subbotina sp.	Rare	Paleocene–Eocene

ture defined by the Zhepure Shan limestone ridges and the distinctive lower-angle slopes (compared with the adjoining limestones) the shale-based unit generates. Thrust repetition of the Zhepure Shan limestones and the overlying clastics is caused by imbrication above a detachment that is folded in the Zhepure Shan syncline and that ramps up-section to the south as it crosses the fold hinge (fig. 2). We reject the member names introduced by Wang et al. (2002), which are those of villages in the Pengqu River Valley 10–15 km away from the section, and introduce the name Shenkeza Formation for the upper 75-m-thick red mudstones and sandstones. This new name is proposed because the red unit is exposed only in the section close to Shenkeza monastery (located about 1 km west of the section; fig. 2) based on our field observations and the distinctive TM image spectral characteristics of these red beds compared with all the other units in the Zhepure Shan. The geological reason these sedimentary rocks should be two separate formations is that a significant unconformity marked by the development of an approximately 4-m-thick paleosol horizon exists between the two units (described in more detail below).

In detail, the upper part of the stratigraphic sequence in the Shenkeza valley section begins with nummulitic grainstones of the uppermost part of the Zhepure Shan Formation. The top of the Zhepure Shan Formation is marked by nummulitic grainstones interbedded with gray shales identical to those of the lower Youxia Formation over a thickness of about 1 m. We interpret this interbedding as indicating a conformable contact. Abundant large foraminifera including *Nummulites atacicus*, *Nummulites globulis*, *Discocyclina dispensa*, *Nummulites* cf. *vedenbergi*, *Assilina globosa*, *Assilina subspinosa* in the topmost nummulitic grainstones (samples Shen 150, 151) immediately below and interbedded with the lowest shales of the Youxia Formation are identical with the assemblage reported by Willems et al. (1996) for the top

of the Zhepure Shan Formation and are compatible with an Ypresian age for the topmost limestones of the Zhepure Shan Formation. The planktonic foraminifera assemblage from shales within the overlying Youxia Formation (described below) makes the younger extension into foraminiferal zone P-10 (and hence a Lutetian age) incompatible with our data. We suggest that the upper part of the Zhepure Shan limestones range from zones P-6 to P-8 and hence extend well up into the Ypresian stage of the Early Eocene.

The Youxia Formation consists of about 105 m of greenish-gray shale intercalated with thin-bedded, green-colored sandstones and rare thin nodular limestone beds (fig. 3). Youxia sandstone beds have tabular geometries and become more numerous, thicker, and coarser grained up-section. Most of the sandstone beds in the unit have scoured bases that display tool marks and flute-type casts. Some are normally graded, and they frequently contain horizontal and ripple cross-lamination. Several of the sandstone beds are hummocky cross-stratified, particularly those in the upper part of the unit.

We interpret the Youxia Formation to have been deposited in an outer-shelf marine environment. Sandstones were deposited from turbid suspension currents, while the interbedded shales were deposited by suspension settling of clay between or following high-energy events. The hummocky cross-stratification, particularly in the thick sands in the upper part of the section, suggests that later deposition occurred within the influence of storm waves (Walker 1979). Some of the thin arenites in the middle of the section may have been deposited as turbidites, but the upper ones are unquestionably storm deposits, and the thinner, finer-grained beds in the middle of the section may be as well.

The age of the Youxia, in contrast to the Zongpubei at Gamba, can be assessed directly from planktonic foraminifera (table 1) found in the shales (sample Shen 90). The most age-diagnostic planktonic foraminifera in the shales of the Youxia For-

mation include *Morozovella lensiformis*, *Morozovella quetra*, *Morozovella aequa*, *Morozovella formosa*, and *Morozovella aragonensis.* Of these, *M. lensiformis*, *M. quetra*, *M. aequa*, and *M. formosa* all have their last appearance datum in planktonic foraminifera zone P-8. The first appearance of *M. aragonensis* is in P-8, with a range extending to P-10. Thus the most consistent biostratigraphic assignment for these shales is P-8, a partial range zone of the late Ypresian extending from 50.8 to 50.4 Ma, according to Berggren et al.'s (1995) timescale.

The green, predominantly shaley sediments of the Youxia Formation are disconformably overlain by the Shenkeza Formation. The Shenkeza, about 75 m thick in this section, consists of mudstone and red shales and interbedded lensoid beds of sandstone. The disconformity on the green arenites of the Youxia Formation is marked by a 25-cm-thick bed of poorly sorted, angular, pebble/cobble-sized material derived from the underlying unit. We interpret this as a paleoregolith immediately overlain by 4 m of red mudstone containing green mottles, angular/blocky pedogenic structures, argillaceous cutans, and slickensides (not of fault origin). We interpret this lowermost Shenkeza mudstone to be a paleovertisol (sensu Mack et al. 1993) that formed during development of a major disconformity. Shenkeza sandstone beds have lenticular geometries, are 1–3 m thick, and are tens to hundreds of meters in width. Individual sandstone beds have scoured bases, fine upward, and contain trough cross-stratification, horizontal lamination, and ripple cross-lamination. The red mudstones within this unit also contain evidence in places for pedogenic modification, including angular/blocky pedogenic structures, argillaceous cutans, and slickensides.

Wang et al. (2002) interpreted the rocks of the red Shenkeza Formation to have been deposited in a shallow marine shelf environment and reported marine microfossils from them. Based on our observations, however, we interpret this unit to represent fluvial channel and floodplain deposits. In addition, because of our identification of a potentially substantial disconformity at the base of the red unit and the overall nonmarine nature of the interval, we consider the late Priabonian age of the upper member reported by Wang et al. (2002) to be highly suspect. This age was based on the presence of calcareous marine nannofossils in the red mudstones, but we suggest that these fossils were all reworked from older marine strata. As such, the unit may be significantly younger than the Late Eocene–Early Oligocene age of the fossils identified

in the unit. This interpretation is supported by the presence of older, reworked lower Tertiary marine microfauna and Mesozoic pollen also identified in it by Wang et al. (2002).

Sedimentary Provenance Studies

In this study, we undertook an integrated approach to determine the provenance of the Tertiary clastics in the Zhepure Shan section since individual provenance techniques have limitations (Humphreys et al. 1991). Our approach maximizes the number of provenance indicators and minimizes the adverse effects of diagenesis and regional variations in lithology and grain size (Bhatia 1983, 1985; Taylor and McLennan 1985; Bhatia and Crook 1986; Roser and Korsch 1986, 1988; McLennan et al. 1990, 1993; Morton 1991).

Sandstone Petrology.   A petrographic study was conducted on seven sandstone samples from the Youxia and Shenkeza Formations and three from the Jidula Formation. This permits a comparison between deposits of the Indian passive margin (Jidula) with potentially early collision-related (Youxia) and later collisional clastic rocks (Shenkeza). Sample stratigraphic positions are shown in figure 3, and locations are listed in table A1 (available in the online edition of the *Journal of Geology* and also from the Data Depository in the *Journal of Geology* office upon request). For consistency and accuracy, 500 points were counted, following the Gazzi-Dickinson point-counting method (Dickinson and Suczek 1979; Ingersoll et al. 1984; Zuffa 1980) whereby sand-sized minerals included within lithic fragments are counted as the mineral phase rather than as the host lithic fragment. Given the fact that some minerals and rock fragments may be extensively altered after diagenesis and low-grade metamorphism, an effort was made to recognize those components and count them as original framework grains. Feldspar was identified on the basis of its relative relief, twinning, cleavage, and characteristic alteration. Point-counting percentages are given in table 2. Plots of these data on conventional triangular compositional diagrams (fig. 4) are used to infer tectonic setting during the deposition of the early Tertiary clastics in the Zhepure Shan region.

In the calcareous sandstones of the Jidula Formation, well-sorted, subrounded to subangular quartz (>50%) dominates over lithic fragments (~2%) and feldspar (~1%). These sandstones contain considerable calcareous matrix (32%–36%). Quartz grains are mostly monocrystalline and show considerable undulosity and strain lamellae.

Table 2.   Framework Grain Mode Parameter of Sandstones from the Lower Tertiary Terrigenous Clastics in the Zhepure Shan Region

Sample	Shen 94	Shen 88	Shen 87	Shen 148	Shen 145	Shen 141	Shen 138	Jul 75	Jul 2	Jul 1
M-quartz	198	242	243	207	197	145	234	302	290	250
P-quartz	67	37	31	5	22	21	13	10	17	11
Plag	29	22	15	14	24	21	16	0	1	0
K-spar	1	4	3	0	2	0	1	8	3	4
V-lithic	55	56	46	17	26	31	9	0	0	0
M-lithic	24	22	16	5	14	18	5	4	0	2
S-lithic	93	95	126	84	102	125	151	9	9	8
Matrix	27	13	10	99	88	92	62	159	164	204
Mica	2	2	3	1	1	1	5	0	1	0
Opaque	3	3	5	66	23	44	3	7	10	19
Unknown	1	4	2	2	1	2	1	1	5	2
P/F	.97	.85	.83	1.00	.92	1.00	.94	0	.25	0

Note.   M-quartz = monocrystalline; P-quartz = polycrystalline; Plag = plagioclase; K-spar = K-feldspar; V-lithic = volcanic; M-lithic = metamorphic; S-lithic = sedimentary; P/F = plagioclase/total feldspar ratio; 500 points counted per sample.

The lack of any common orientation to the strain lamellae suggests that they were strained in the source area. Inclusions of mica, rutile, and zircon within quartz are observed. Metamorphic and sedimentary lithics are the major rock fragments, and no volcanic detritus has been observed. Feldspar is a minor phase, only ~1% of the total framework grains; most are K-feldspar. Minor heavy detrital phases include zircon, rutile, tourmaline, ilmenite, and magnetite. No Cr-rich spinel was observed. The dominance of monocrystalline, subangular-to-subrounded quartz grains, the presence of minor potassium feldspar with little to no plagioclase, and the paucity of lithic fragments suggest derivation from cratonic continental sources.

Green sandstones in the Youxia Formation are dominated by quartz grains (monocrystalline and polycrystalline) and lithic fragments, often poorly sorted with angular to subangular shapes; well-rounded grains are rarely observed. Although most monocrystalline quartz grains (42%–51%) show undulose extinction, a few uniformly extinguishing quartz grains are conspicuously clear, suggestive of a volcanic origin. Lithic fragments are abundant and constitute approximately 38% of total framework grains. Textures indicate that volcanic rock fragments are commonly intermediate or silicic in composition and consist of plagioclase phenocrysts in a fine-grained or aphanitic groundmass. Sedimentary lithics are dominantly micritic to sparitic limestone and chert and sporadic siltstone and shale. Quartz-mica aggregates and fine schists are the major constituents of metamorphic lithics. Feldspar (4%–6%) is common, and plagioclase is the dominant feldspar in the green sandstones, with the ratios of plagioclase to total feldspar >0.83 (table 2). Feldspar grains are typically fresh and unaltered and range from large euhedral crystals to suban-

gular broken crystals commonly showing albite-Carlsbad twinning. The dominant accessory minerals include muscovite, chlorite, and opaque minerals (magnetite and Cr-rich spinel) along with less common zircon, apatite, sphene, and rutile.

In the Shenkeza Formation, the compositions of the red sandstones are similar to the Youxia green sandstones, consisting primarily of quartz (42%–50%), rock fragments (21%–36%), and minor feldspar (~5%). However, the red sandstones are very fine to fine grained and contain more than 10% matrix. There is a significantly higher content of opaque minerals (magnetite and Cr-rich spinel) and lower contents of polycrystalline quartz and volcanic lithic compared with the Youxia sandstones.

Interpretation of Sandstone Modes.   The compositions of sandstones in the Jidula Formation are dominantly monocrystalline quartz with minor rock fragments while those in the Youxia and Shenkeza Formations have a much larger content of rock fragments, some of which are volcanic. The preservation of unaltered and euhedral plagioclase in the Youxia and Shenkeza sandstones suggests rapid erosion, transport, and burial. These differences suggest a significant provenance change during the deposition of lower Tertiary clastics in the Tingri region. To visualize the variations in sand composition and to help interpret the tectonic provenance of these sandstones, the relative contents of quartz, feldspar, and rock fragment have been plotted on the Q_tFL and $QmFL_t$ ternary diagrams (fig. 4) together with the fields for the tectonic settings of Dickinson (1985).

These figures illustrate that the quartz-rich, lithic-poor Jidula sandstones plot at the boundary of the continental block and recycled orogen provinces on the Q_tFL diagram and in the continental block province on the Q_mFL_t diagram, while the
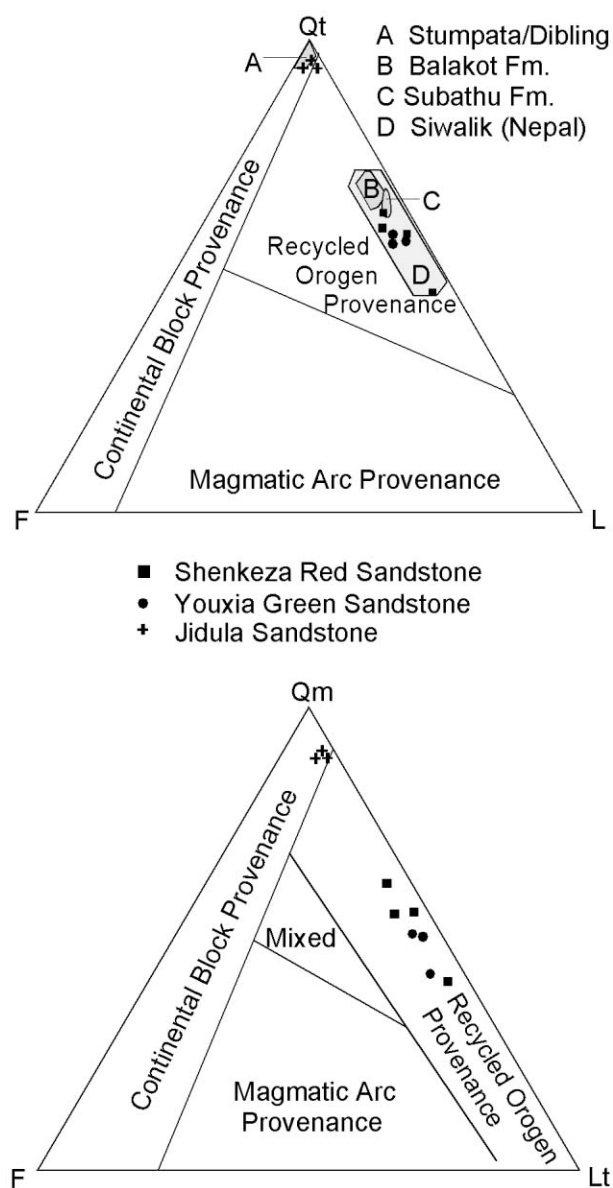
Figure 4. Detrital mode plot of lower Tertiary sandstones in the Tingri region. Tectonic fields are from Dickinson (1985). Fields shown of other related Himalayan sandstones are from Garzanti et al. (1996).

relatively quartz-poor, lithic-rich Youxia and Shenkeza sandstones plot in the recycled orogenic provenance. The fact that all Jidula sandstones plot in the continental block area on the Q_mFL_t plot suggests strongly that they were ultimately derived from a cratonic interior, consistent with the common presence of an ultrastable dense mineral assemblage (zircon, rutile, and tourmaline). In contrast, abundant volcanic rock fragments and the presence of Cr-rich spinel in the Youxia and Shen-

keza sandstones point to a volcanic setting. They consistently plot in the recycled orogen areas on the Q_mFL_t plot. We think this influx of abundant immature detritus was related to the arrival of the subduction complex of the Gangdise arc-trench system at this segment of the northern Indian passive margin and is the first harbinger of synorogenic foreland-basin deposition of the India-Asia collision in the Zhepure Shan region.

Sandstone and Shale Geochemistry

Studies (Bhatia and Crook 1986; Cullers et al. 1988; McLennan et al. 1990, 1993) have shown that certain trace elements (e.g., Zr, Sc, Nb, Ga) are virtually insoluble during weathering, erosion, and transport and are transported nearly quantitatively from sources in various tectonic settings into terrigenous clastic sediments. A few ratios of major oxides are also relatively constant from source to sink (Bhatia 1983, 1985; Roser and Korsch 1988; Hayashi et al. 1997; Rahman and Faupl 2003). Accordingly, whole-rock geochemical compositions of sedimentary rocks bear a relationship to the composition of the source rocks and have often been used successfully to constrain the specific tectonic affinities of the sites of provenance of various siliciclastic sediments. Given the fact that the less resistant phases are labile and modified with burial and metamorphism (Morton 1991), the study of geochemical compositions of clastic sediments complements detrital modal analyses. Geochemical analyses of the shales and sandstones from the Jidula, Youxia, and Shenkeza formations are listed in table A2 (available in the online edition of the *Journal of Geology* and also from the Data Depository in the *Journal of Geology* office upon request).

Major Elements. The effect of weathering processes on sedimentary rock sources can be assessed using the chemical index of alteration (CIA; Nesbitt and Young 1982) and to quantify the source weathering history (e.g., McLennan et al. 1993; Bock et al. 1998; Young et al. 1998; Young 2002). The CIA is defined as molecular proportions: $CIA = 100 \times Al_2O_3/(Al_2O_3 + CaO^* + Na_2O + K_2O)$, where CaO^* is CaO in silicate minerals, as opposed to carbonates or phosphates. Details of the CaO correction for bulk-rock chemistry are given by McLennan et al. (1993). Sandstones of Jidula Formation have higher CIA values than those of the Youxia and Shenkeza Formations, indicating a more intense source weathering history or incorporation of material from mature sediments (fig. 5). The Youxia and Shenkeza sandstones have the lowest CIA values (53–54), close to values of ~50 char-
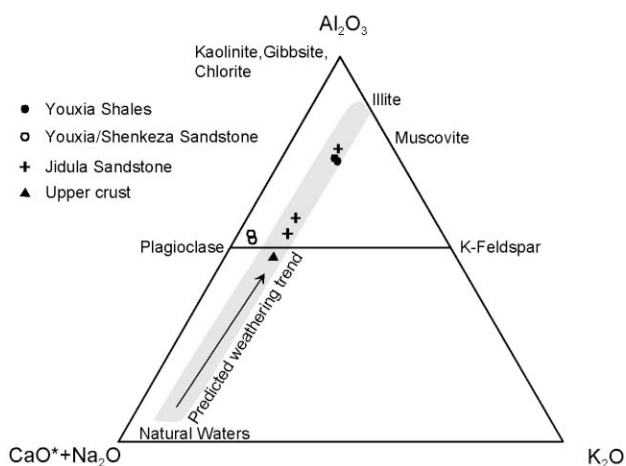
Figure 5. Chemical index of alteration ternary plot of lower Tertiary clastics in the Tingri region. Modified after Bock et al. (1998). The enrichment in Al_2O_3 and depletion of $CaO^* + Na_2O + K_2O$ on this plot reflects the degree of chemical weathering to which the materials have been subjected. Three analyses of the Jidula Formation define a linear trend encompassed in the predicted weathering trend for the average upper crustal composition, while those of the Youxia Formation do not follow the predicted weathering trend, indicating processes in addition to the weathering have affected the Youxia sediments.

acteristic of fresh granites and rhyolites. This suggests limited chemical weathering for Youxia and Shenkeza Formation sediments, consistent with the observations of detrital feldspar grains, especially less stable plagioclase, and abundant rock fragments in the thin sections. In the ternary plot of $Al_2O_3 - (CaO^* + Na_2O) - K_2O$ (fig. 5), three analyses of the Jidula sandstones display a range of CIA values (measured by height on the triangle) from about 54 to 77 and follow a linear trend parallel with the $Al_2O_3 - (CaO^* + Na_2O)$ join. According to Nesbitt and Young (1982), this trend is produced exclusively by weathering processes. Four analyses of Youxia and Shenkeza Formation sediments do not follow the linear trend (fig. 5) of the Jidula Formation, probably suggesting the mixing of provenance components from different source areas (McLennan et al. 1993).

Detrital sediments from the Youxia and Shenkeza Formations define a linear trend on a SiO_2-Al_2O_3 graph (fig. 6), with shales of the Youxia Formation containing lower SiO_2 and correspondingly higher Al_2O_3. Three analyses in the Jidula Formation do not follow this linear trend, possibly indicative of a different provenance. In particular, Jul 75

and Jul 2 have significantly higher SiO_2/Al_2O_3 ratios than those from the Youxia and Shenkeza sandstones (fig. 6). This may be explained by the textural maturity in the Jidula sandstones and confirms that quartz is significantly more abundant than primary clay-sized material and labile framework grains (plagioclase and rock fragments) in these quartzose sandstones, resulting in an elevation of the SiO_2/Al_2O_3 ratio (McLennan et al. 1993). The K_2O/Na_2O ratios of the Youxia and Shenkeza sandstones (0.22 and 0.27) are significantly different from those of the Jidula sandstones (2.59 and 0.95; fig. 6). Because sands from volcanically active settings commonly have K_2O/Na_2O <1, whereas sands from a passive margins draining continents exhibit ratios >1 (McLennan et al. 1990), the differing ratios indicate a significant provenance change between the sandstones of the Jidula and Youxia Formations. The relative enrichments of Mg, Mn, Ni, and V in the Youxia and Shenkeza sandstones compared with those in the Jidula Formation also suggest that there was a mafic/ultramafic component in the source, such as that associated with an ophiolite-obduction event (McLennan et al. 1990; Bock et al. 1998). This is in agreement with the observations described above: well-sorted and subrounded-subangular quartz are the primary framework grains in the Jidula sandstones, whereas there are significant amounts of labile rock fragments in the Youxia and Shenkeza sandstones.

The Jidula and the Youxia and Shenkeza formations combined define two linear trends in the Al_2O_3 versus TiO_2 plot (fig. 6). The Jidula Formation has Al_2O_3/TiO_2 <5, whereas the ratios of the Youxia and Shenkeza Formations vary from 16.9 to 20.7. The relatively constant Al_2O_3/TiO_2 ratios in the Youxia and Shenkeza Formations confirm that the fractionation of Al and Ti is minimal between associated sandstones and shales/mudstones (Hayashi et al. 1997; Rahman and Faupl 2003). Hayashi et al. (1997) suggested that the Al_2O_3/TiO_2 ratio of a sedimentary rock could be essentially the same as that of its source rock and may be used as a provenance indicator. If this is the case, the ratios of Al_2O_3/TiO_2 in the Youxia and Shenkeza Formations (16.9–20.7) are comparable to those for intermediate igneous rocks (Holland 1984). Representative geochemical analyses for the Xigaze ophiolite show Al_2O_3/TiO_2 ratios mostly between 16.6 and 21.5 (Pearce and Deng 1988), and the sandstones in the Xigaze fore-arc basin have similar Al_2O_3/TiO_2 ratios (typically ~18; Durr 1996), so it is likely that both the Xigaze group and the Youxia Formation share a common source, most likely, the granodiorites and andesitic volcanics of the Gang-
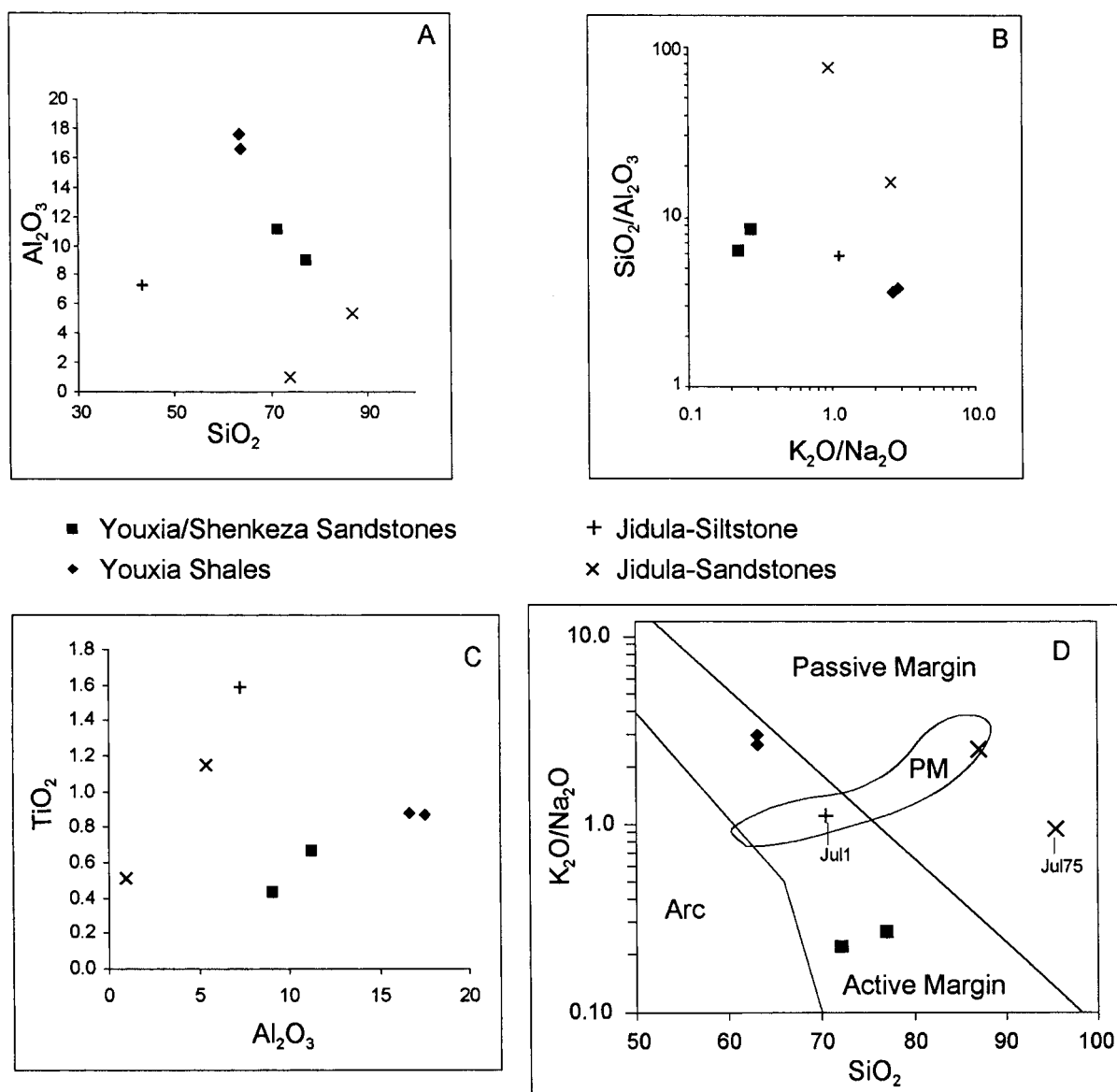
Figure 6. Geochemical plots of the lower Tertiary clastics in the Tingri region. *A*, Al_2O_3 versus SiO_2. *B*, SiO_2/Al_2O_3 versus K_2O/Na_2O. *C*, TiO_2 versus Al_2O_3. *D*, K_2O/Na_2O versus SiO_2. Tectonic setting fields for *D* are from Roser and Korsch (1986), with addition of passive margin field from McLennan et al. (1990). In *D*, Jul 1 and Jul 75 are recalculated to 100% CaO and are volatile free because of significantly high calcite contents.

dese arc to the north. The lower Al_2O_3/TiO_2 ratios in the Jidula Formation point to a different provenance; relatively low Al abundances may reflect a combination of weathering and reworking. A greater degree of recycling has eliminated most labile detrital minerals with high Al contents. Accordingly, the Jidula Formation was likely derived from a cratonic interior, specifically the Indian continent to the south.

Trace Elements. Certain trace elements (e.g., Zr, Th, Sc, Nb, Ga) and rare earth elements (REE) are considered to be essentially constant in abundance because of their relatively low solubilities during weathering and low residence time in seawater (Bhatia and Crook 1986; Cullers et al. 1988; McLennan et al. 1990, 1993). They are transferred quantitatively into terrigenous sediments during sedimentation and record the signature of parent
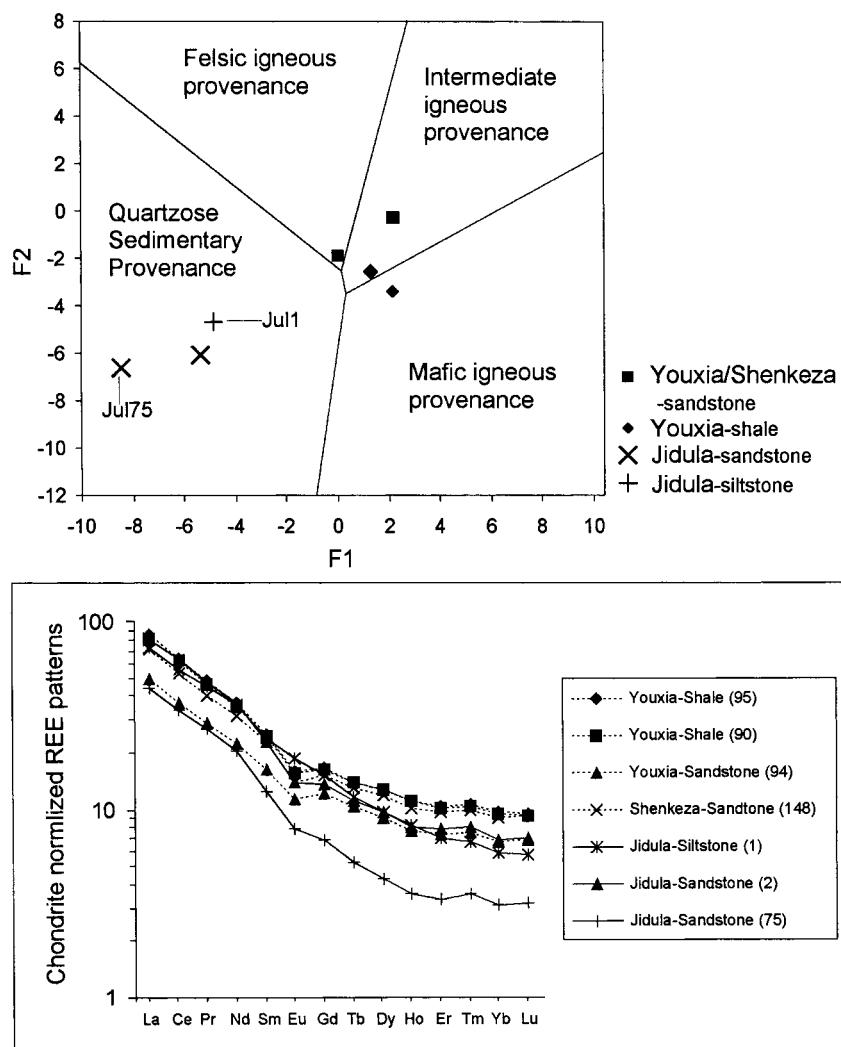
Figure 7. Geochemical plots of the lower Tertiary clastics in the Tingri region. *Top,* Provenance discrimination diagram. Tectonic setting fields are from Roser and Korsch (1988). Jul 1 and Jul 75 are recalculated to 100% CaO and are volatile free because of significantly high calcite contents. *Bottom,* Chondrite-normalized rare earth element patterns; chondritic values are those of Taylor and McLennan (1985).

materials (Bhatia and Crook 1986; McLennan et al. 1990).

Zr contents in the Jidula Formation rocks (377–567 ppm) are significantly higher than those in the Youxia and Shenkeza Formations (172–282 ppm). High Zr abundance generally is caused by zircon grains (Hiscott 1984), a common heavy mineral in most mature sands derived from old continental rocks. Cu contents in the Jidula Formation (0–6 ppm) are significantly less than those in the Youxia and Shenkeza Formations (14–91 ppm). Since Cu is generally found in sulfide minerals, commonly present in volcanic rocks (Hiscott 1984), the relative enrichment of Cu in the Youxia and Shenkeza

Formations provides further evidence for significant amounts of volcanic lithologies in the source area.

In the chondrite-normalized REE diagram (fig. 7, *bottom*), the Jidula Formation has light REE (LREE)–enriched and heavy REE (HREE)–depleted patterns (LREE/HREE from 8.9 to 11.6, $La_n/Yb_n = 11.42$–14.34). Eu/Eu* values range from 0.79 to 0.98, which may by themselves suggest a source from the undifferentiated arc or differentiated arc (McLennan et al. 1990, 1993). In the Jidula Formation, abundant zircon and low total REE abundances may have significantly affected the chondrite-normalized REE patterns (Taylor and
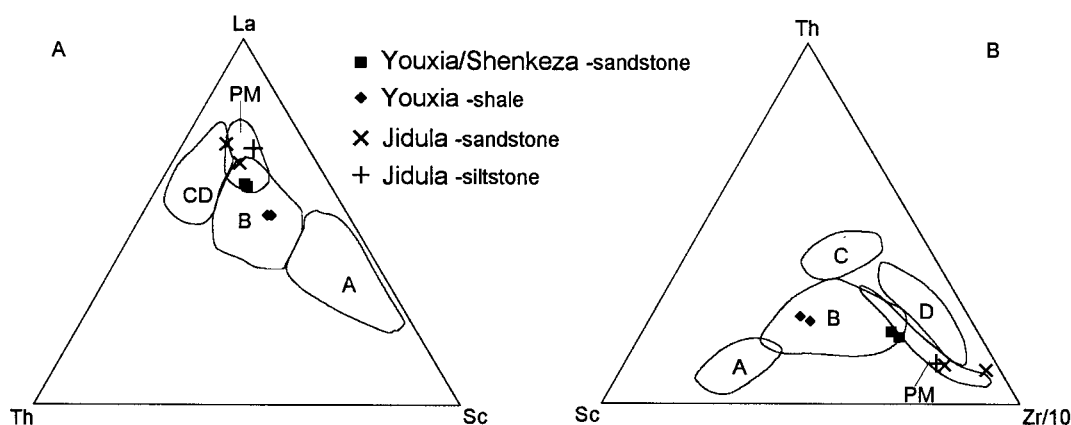
Figure 8. Tectonic discrimination plots from Bhatia and Crook (1986). *A*, La-Th-Sc ternary. *B*, Th-Sc-Zr/10 ternary. Fields: *A* = oceanic island arc, *B* = continental island arc, *C* = active continental margin, *D* = passive margin, *PM* = passive margin field from McLennan et al. (1990).

McLennan 1985). On the basis of the other geochemical and petrologic data, it is unlikely that the Jidula Formation was derived from a volcanic arc. In contrast, chondrite-normalized REE distribution patterns of the Youxia and Shenkeza Formations show LREE enrichment trends with slightly depleted HREE (LREE/HREE = 6.3–7.7, La_n/Yb_n = 7.3–8.8) and slightly negative Eu anomalies (Eu/Eu^* = 0.74–0.81). These features, coupled with different La/Sc, Nb/Y, Gd_n/Yb_n ratios, and Hf and Cs abundances, suggest a significant provenance change between the sandstones of the Jidula and Youxia and Shenkeza Formations. The close similarity in the average La/Sc, La_n/Yb_n, Eu/Eu^*, and total LREE/HREE ratios of the Youxia and Shenkeza Formations to the continental island arc values (Bhatia 1985; Bhatia and Crook 1986) supports the above inference and suggests a source from andesitic-felsic volcanic rocks within a continental volcanic-arc tectonic setting for the Eocene clastic rocks in the Tingri region.

Geochemical Discrimination of Tectonic Environment. In the K_2O/Na_2O-SiO_2 discrimination diagram (Roser and Korsch 1986), four analyses of the Youxia and Shenkeza Formations fall into the active continental margin field (fig. 6). Jidula Formation samples fall into or close to the passive margin field. Using major oxides as variables, the discriminant functions of Roser and Korsch (1988) were designed to distinguish between sediments from four provenances: mafic, intermediate, and felsic igneous rocks and quartzose sedimentary materials. Four analyses from the Youxia and Shenkeza Formations plot in the mafic-felsic igneous

provenances, while Jidula Formation samples plot in the quartzose sedimentary provenance.

Bhatia and Crook (1986) developed a series of discriminant diagrams based on trace element ratios from Paleozoic sandstones to allow distinction between oceanic island arc, continental island arc, active continental margin, and passive continental margin environments of deposition. On the Th-Sc-La and Th-Sc-Zr/10 ternary diagrams (fig. 8), the Youxia and Shenkeza Formations consistently fall in the field of continental island arcs, indicating that there was a significant volcanic arc source for the Youxia and Shenkeza clastic sediments. The Jidula Formation samples plot close to or within the passive margin field (fig. 8).

In summary, geochemical and petrographic data are consistent with the interpretation that the Jidula Formation is dominated by mature, cratonic detritus deposited on the Indian passive margin. The relatively enriched elements (Mg, Mn, Ni, and V) and high Cu and Al_2O_3/TiO_2 values in the Youxia and Shenkeza sandstones indicate a volcanic arc provenance, most likely derived from andesitic-felsic volcanic rocks in a continental volcanic-arc tectonic setting.

Chemical Compositions of Cr-Rich Spinel

A large number of heavy mineral species with specific gravity >2.80 occur in sandstones, many of which are source-diagnostic (Morton 1985, 1991; Evans and Mange-Rajetzky 1991; Mange and Maurer 1992). Among these, chromium-rich spinel is unique in terms of occurrence and tectonic sig-
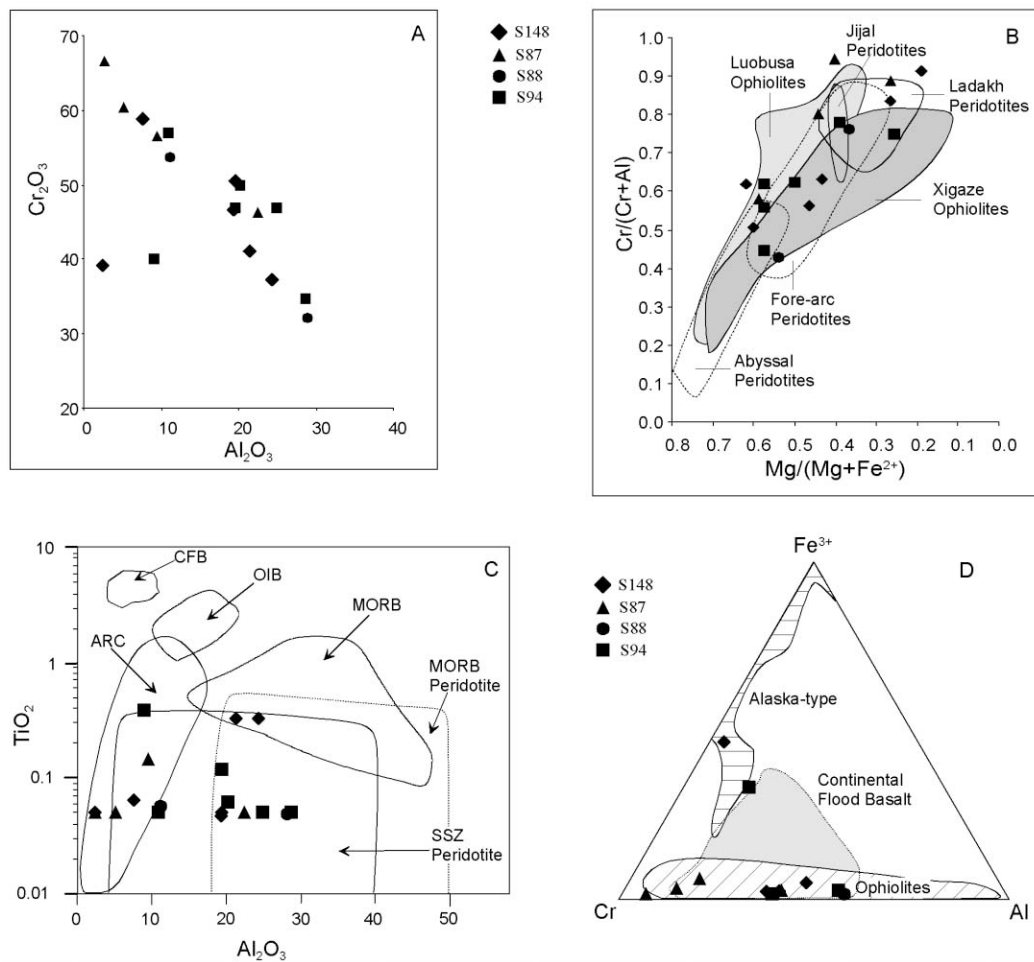
Figure 9. Geochemical plots of Cr-rich spinels from the Youxia and Shenkeza sandstones. *A*, Cr_2O_3 versus Al_2O_3. *B*, Cr number (Cr/[Cr + Al]) versus Mg number (Mg/[Mg + Fe^{2+}]). Fields displayed are abyssal peridotites from Bryndzia and Wood (1990), fore-arc peridotites from Parkinson and Pearce (1998), Jijal peridotites and Ladakh peridotites from Rolland et al. (2002), Luobusa ophiolites from Zhou et al. (1996), and Xigaze ophiolites from Wang et al. (2000). *C*, TiO_2 versus Al_2O_3. Fields displayed are from Kamenetsky et al. (2001): *CFB* = continental flood basalt, *OIB* = oceanic island basalt, *MORB* = mid-ocean ridge basalt, *ARC* = volcanic island arc, *SSZ* = suprasubduction zone. *D*, Cr-Al-Fe^{3+} ternary plot (12 points with valid Fe^{3+} shown). Fields displayed are from Cookenboo et al. (1997).

nificance because its composition is sensitive to the chemical history of the magma from which it was derived (Irvine 1967; Roeder 1994). The presence of Cr-rich spinels in sedimentary rocks of a basin in or adjacent to an orogenic belt is generally interpreted as an indicator of derivation from ophiolitic peridotites (Pober and Faupl 1988; Cookenboo et al. 1997; Ganssloser 1999; Lee 1999; Najman and Garzanti 2000; Wang et al. 2000), but volcanic sources can also be significant, including hotspot/flood basalts (Barnes and Roeder 2001; Kamenetsky et al. 2001; Zhu et al. 2004).

Dark brown to dark reddish-brown spinels were found in the Youxia and Shenkeza sandstones but

not in the Jidula sandstones. Microprobe analyses of these detrital spinels are shown in table A3 (available in the online edition of the *Journal of Geology* and also from the Data Depository in the *Journal of Geology* office upon request). There is an inverse relationship between Cr and Al contents (fig. 9*A*), which may be indicative of different degrees of partial melting in the mantle (Dick and Bullen 1984). Spinel grains show no obvious signs of zoning in line scans. This suggests that (1) parental lavas had undergone little or no magma mixing or significant crustal assimilation (Allan et al. 1988), (2) there was no extensive subsolidus reequilibration between spinels and other silicate

minerals (Scowen et al. 1991), and (3) no major metamorphic event occurred after these spinels crystallized. There is no significant variation in the chemistry of Cr-rich spinels within these samples as a function of stratigraphic position.

Source of Cr-Rich Spinels

In terms of origin and tectonic setting, Cr-rich spinels from various types of ultramafic and mafic complexes can be discriminated using major-element abundances (Irvine 1967; Dick and Bullen 1984; Barnes and Roeder 2001; Kamenetsky et al. 2001). Overlaps among various tectonic settings on some plots (Dick and Bullen 1984), however, are common because only selected aspects of the total chemical variation are reflected in the binary plot of individual elements (Cookenboo et al. 1997). Multiple combinations of major elements, therefore, should be considered to determine the possible parental magma of the studied spinels.

Most spinel-bearing peridotites have spinels with low TiO_2 abundances, whereas volcanic spinels with TiO_2 <0.2 wt% are uncommon (Kamenetsky et al. 2001). Lenaz et al. (2000) set a compositional boundary between peridotitic and volcanic spinels at $TiO_2 = 0.2$ wt%. Because 15 of 18 analyses have TiO_2 contents <0.2 and most are near or below the detection limit of ~0.05 wt% (fig. 9C), the detrital spinels from the Youxia and Shenkeza Formations were most likely derived from mantle (ophiolitic) peridotites.

The detrital spinels in the Youxia and Shenkeza sandstones have a Cr number (e.g., Cr/[Cr + Al]) between 0.43 and 0.94 and a Mg number $(Mg/[Mg + Fe^{2+}])$ between 0.19 and 0.62. These compositions, according to the classifications of Dick and Bullen (1984), correspond best with spinels in Type II peridotites, which are transitional from volcanic arc to typical oceanic crust (Najman and Garzanti 2000). There is a strong negative correlation between Cr number and Mg number (fig. 9B), a typical Cr-Al trend (Barnes and Roeder 2001), probably corresponding to spinels equilibrating with olivine of constant composition at constant temperature (Irvine 1967; Roeder 1994). The spinels vary from Al-rich spinels (sensu stricto) to Cr-rich chromites (sensu stricto). In the conventional fields (fig. 9B) of tectonic settings for spinels (Dick and Bullen 1984; Barnes and Roeder 2001), our data plot in the field of fore-arc peridotites.

In the plot of TiO_2 versus Al_2O_3 (fig. 9C), assuming TiO_2 is ~0.05 for spinels with TiO_2 abundances <0.05, comparison of our data with the compositional fields of spinels from well-studied tectonic

settings demonstrates that detrital spinels in the Youxia and Shenkeza Formations do not fall in the linear trend defined by spinels from continental flood basalts (CFB), oceanic island basalts (OIB), and mid-ocean ridge basalts (MORB) and are best assigned to source rocks from suprasubduction zone mantle peridotites (Kamenetsky et al. 2001). Hotspot-related basalts such as the Deccan Traps did not significantly contribute to the Youxia and Shenkeza sandstones because Deccan Trap spinels commonly have >1% TiO_2 and relatively constant Cr number values mostly between 0.6 and 0.7 (Najman and Garzanti 2000; Barnes and Roeder 2001).

Six of 18 spinel analyses have negative ferric iron values (table A3). All Fe^{3+} values were determined by assuming stoichiometry with three cations per four O atoms, following the methods of Barnes and Roeder (2001), and the negative Fe^{3+} values indicate these spinels are nonstoichiometric. This may be good evidence that an arc complex is a significant source for the spinels in the Youxia and Shenkeza sandstones because nonstoichiometry is a common feature for Cr-rich spinels from primitive subduction-related magmatic suites, such as Ti-poor tholeiite from Hunter Fracture Zone and high-Ca boninites from the Tonga Trench (Kamperman et al. 1996). Ten of 12 analyses with calculated Fe_2O_3 >0 have $Fe^{3+}/(Fe^{3+} + Al + Cr)$ <0.1, plotting in the field of ophiolites in the Fe^{3+}-Al-Cr ternary diagram (fig. 9D).

Considered together, the plots of Mg number versus Cr number, TiO_2 versus Al_2O_3, and Fe^{3+}-Al-Cr demonstrate that the compositional range of the detrital spinels in the Youxia and Shenkeza sandstones closely matches that of spinels from suprasubduction-related magmatic rocks and excludes OIB, MORB, and CFB as major sediment sources. Also shown (fig. 9B) are spinels from Luobusa ophiolites (Zhou et al. 1996) and Xigaze ophiolites (Wang et al. 2000) in southern Tibet and Kohistan-Ladakh mafic-ultramafic suites in the NW Himalaya (Jan and Windley 1990; Jan et al. 1992; Rolland et al. 2002). It is clear that there are significant overlaps between spinels from Youxia and Shenkeza sandstones and those from the arc and ophiolitic rocks in this plot. Furthermore, the compositions of detrital spinels in the Youxia and Shenkeza sandstones are very similar to those of the Chulung La Formation in Zanskar (Garzanti et al. 1987, 1996); the Subathu Formation (Najman and Garzanti 2000) in Himachal Pradesh, northern India; and the Murree redbeds (Bossart and Ottiger 1989; Critelli and Garzanti 1994) in the Hazara-Kashmir Syntaxis, northern Pakistan, which are syncollisional clastics derived from the obducting

Asian (Gangdise) arc-trench system. We conclude that the detrital spinels in the Youxia and Shenkeza sandstones were most likely derived from arc and ophiolitic igneous sequences of the Yarlung-Zangbo suture zone and Gangdise arc to the north.

Discussion

Regional Correlatives of Lower Tertiary Clastic Rocks. Sandstones similar to the Youxia and Shenkeza sandstones occur in sedimentary sequences in the Himalayan foreland basin (fig. 10). These include the upper part of Subathu Formation (perhaps Middle Eocene) and younger Dagshai Formation in northern India (Najman and Garzanti 2000) and the Middle Eocene–Miocene Murree Formation in northern Pakistan (Bossart and Ottiger 1989; Critelli and Garzanti 1994; Garzanti et al. 1996). Detrital modes show that those sandstones were de-

rived from the "recycled orogen" setting (fig. 4), characterized by significant amounts of immature framework grains (plagioclase, felsitic to microlitic volcanic rock fragments, serpentine schist lithics) and common spinels. The close similarity in the compositions of Cr-rich spinels also suggests that there was a common source for the lithic-rich sandstones. This is very different from the underlying Paleocene quartzose arenites intercalated within mainly shelf carbonate deposited on the passive margin of the Indian continent, including the Stumpata and Dibling Formations in Zanskar (Garzanti et al. 1987), the Patala Formation in Hazara-Kashmir (Bossart and Ottiger 1989), and the Jidula Formation in southern Tibet (Willems and Zhang 1993; Willems et al. 1996). The detrital modes of the quartzose arenites consistently plot in or close to the "continental block" provenance field (fig. 4), characterized by abundant well-sorted monocrys-

Epoch	Stage	Age (Ma)	Hazara-Kashmir	Zanskar	Himachal Pradesh (N. India)	Tingri
Eocene		33.7				
	Priabonian		Balakot Fm.			Shenkeza Fm.
		36.9				?
	Bartonian					
		41.4				
	Lutetian			Chulung La Fm. & Kong Fm.	Subathu Fm. (clastics)	
		49.0		P8	?	Youxia Fm. P8
	Ypresian			Kesi Fm.	Subathu Fm. (limestones)	
		54.7	Patala Fm.			
Paleocene	Thanetian			Dibling Fm. & Shinge La Fm.	?	Zhepure Shan Fm.
		57.9	Lockhart Fm.			
	Selandian					
		61.0				
	Danian			Stumpata Fm.		Jidula Fm.

Figure 10. Comparison of stratigraphic columns of the early Himalayan foreland basin. Hazara-Kashmir (Bossart and Ottiger 1989, modified by Najman et al. 2002), Zanskar (Garzanti et al. 1987, 1996), Himachal Pradesh (Najman and Garzanti 2000), and Tingri, southern Tibet (this study). Timescale after Berggren et al. (1995); stages are not proportionately scaled to numerical age ranges. A question mark indicates significant uncertainty for the age of the boundary or the base/top of section. Age of the Shenkeza Formation is not determined.

talline quartz and a general lack of volcanic lithics, plagioclase, and Cr-rich spinels.

Therefore, the lower Tertiary siliciclastic sequences in the Himalaya record an abrupt change in provenance: mature, quartz-rich sandstones (Jidula, Stumpata, Dibling, and Patala formations) indicate a provenance from the basement rocks of Indian continent to the south while immature, lithic-rich sandstones (Youxia, Shenkeza, Subathu, and Murree Formations) were most likely derived from the obducting Trans-Himalayan arc-trench system to the north. This temporal evolution is consistent with the expected sequence of tectonosedimentary episodes when an arc collides with a passive continental margin (e.g., Rowley and Kidd 1981). Quartzose sandstones derived from the craton are episodically deposited on the passive margin. The start of collision is marked by the deposition of clastics containing volcanic and ophiolitic detritus, which reflects the arrival of the arc-trench system onto the outer parts of the passive margin.

Timing of Indian-Asian Collision in Southern Tibet. As outlined in the "Introduction," precise dating of the age of initiation of collision between India and Asia is still quite poorly determined, reflecting the different and generally indirect approaches that have been used to date it (Najman et al. 1997, 2001, 2002; de Sigoyer et al. 2000, 2001; Searle 2001; Clift et al. 2002; Wan et al. 2002; Wang et al. 2002). Rowley (1996) reviewed data and arguments regarding the age of initiation of the India-Asia collision before 1996, and we review below various data reported more recently than this.

Collisions between an arc and passive margin are associated with marked changes in patterns of subsidence and sedimentation, particularly along the passive margin side of the orogen. Therefore, the sharp change of the sedimentary compositions between the times of deposition of the Zhepure Shan Formation and Youxia Formation in the Zhepure Shan provides a time constraint on the start of collision of India with Asia in southern Tibet. The 1500-m-thick, well-exposed marine stratigraphy of the Zhepure Shan west of Tingri, southern Tibet, shows evidence for continuous sedimentation along the northern passive-type continental margin of the Indian continent from at least late Albian to Ypresian time (Willems et al. 1996). This suggests that collision did not affect this part of the shelf until the late Ypresian, because the persistent slow subsidence recorded by the Zhepure Shan Formation deposition is consistent only with thermally driven, passive-type margin subsidence (Rowley 1998). The conformable contact between the Youxia and Zhepure Shan formations marks the

transition from a passive margin carbonate platform (Willems et al. 1996) to a collisional foredeep, exhibiting a compositional change similar to that observed in Zanskar (Garzanti et al. 1987). Samples of the topmost nummulitic grainstones of the Zhepure Shan Formation contain a well-preserved assemblage constraining the age of this transition as correlative with planktonic foram zone 8 of late Ypresian age. According to Berggren et al. (1995, p. 153) zone P-8 has an estimated range from 50.8 to 50.4 Ma. This places the age of initiation of the collision at about 50.6 Ma. This assemblage contrasts markedly with the late early Lutetian to Bartonian age (47–37 Ma) reported by Wang et al. (2002). The faunal assemblage of the Youxia Formation reported above indicates an age slightly older than the early Lutetian age of the top of the Zhepure Shan Formation reported by Willems et al. (1996), which makes the conclusion derived by Rowley (1998) that collision postdated the early Lutetian no longer tenable.

Stratigraphic data in the Zanskar region, NW Himalaya, suggest that there the age of the start of the India-Asia collision also occurs within zone P-8 and hence also at about 50.6 Ma (Garzanti et al. 1987). Other less well-constrained sections of peripheral foreland basin strata in Pakistan and northern India (Bossart and Ottiger 1989; DeCelles et al. 1998; Najman and Garzanti 2000) and in the Indus Molasse (Clift et al. 2002) are, so far as is known, consistent with this age.

Recently, de Sigoyer et al. (2000) suggested that the age of the eclogite facies metamorphism in the Tso Morari area at 55 ± 6 Ma by U/Pb, Lu/Hf, and Sm/Nd methods constrained the age of Indian continental margin subduction beneath the Asian margin and hence collision (de Sigoyer et al. 2000; Guillot et al. 2003). Subduction of Indian continental crust, converging with Asia at a velocity of about 100 km/m.yr. appropriate for this time interval to depths equivalent to >2.5 GPa (>80 km), would have taken less than about 1.5 m.yr. Within uncertainty, this age is identical with the stratigraphic estimate in the Zanskar area. The Kesi, Kong, and Chulung La Formations in the Zanskar Himalayas (Garzanti et al. 1987) hence remain the best data to constrain the age of initiation of the India-Asia collision in the western Himalaya. Taken together, these data imply extremely limited diachroneity for the age of initiation of the collision from west to east along the suture.

Based on stratigraphic, sedimentologic, and paleontologic evidence, Yin and Harrison (2000) and Wan et al. (2002) argue that the collision of the India and Lhasa continental block was initiated at the

Cretaceous-Paleocene boundary time (~65 Ma) in southern Tibet. However, our data from the Jidula Formation of Zhepure Shan indicate that passive margin deposition persisted without interruption from the Late Cretaceous through the Paleocene and into the Early Eocene. This is demonstrated by the relatively thin siliciclastic succession of the Jidula Formation, the return to carbonate shelf deposition in the overlying Zhepure Shan Formation, and the dominance of mature, quartzose sandstones with an ultrastable heavy mineral assemblage (zircon, rutile, tourmaline) and lack of any north-derived synorogenic components (Cr-rich spinels, abundant labile rock fragments). The clear absence of any signal in both the subsidence history (Rowley 1998) and in details of the provenance of the Late Cretaceous and Paleocene sediments in the Zhepure Shan makes a 65-Ma collision initiation age highly improbable.

Allen et al. (2001) proposed that the Paleocene-Eocene Nummulite limestones of the Western Alps were deposited on the periphery and under the influence of the initial subsidence of the Alpine collisional foreland basin. We point out that application of this model to the lithologically similar Himalayan Nummulitic limestones of the same age is inappropriate because of the much faster convergence rate between India and Asia; at 15 cm/yr, the depositional site along the Indian passive margin would have been underthrust long before completion of the ~10-Ma duration of limestone sedimentation documented in both the Zanskar and Zhepure Shan sections. The subsidence history elucidated by Rowley (1998) shows, unlike the Alps, no detectable increase in subsidence rates through the Paleocene-Eocene limestone deposition.

Estimates of the age of the start of collision before 1995 frequently cited an age of 50 Ma based primarily on the time of rapid decrease in convergence velocity from >10 to 5 cm/yr between India and Asia (Patriat and Achache 1984; Richter et al. 1992). This marked decrease occurs between chrons 21 and 20, which, based on Berggren et al.'s (1995) timescale, is now dated at 47.2 Ma. Hence, the current direct dating of the start of collision does not correlate in time with the slow down. This implies, and not unreasonably so, that there was ~300–400 km of continent-continent convergence between India and Asia before the convergence rate was affected.

Conclusions

Lower Tertiary sediments well exposed in the Zhepure Shan region, south-central Tibet, represent one of the few well-preserved stratigraphic sections containing the passive margin–peripheral foredeep basin clastic facies transition in the Himalaya. The petrography and geochemistry of the Jidula, Youxia, and Shenkeza formations provide strong data to reconstruct the early tectonic evolution of the Himalaya in south-central Tibet during the early Tertiary. Sedimentation in the older Jidula Formation of Danian age is dominated by mature detritus and closely compares geochemically with sediments deposited on a passive continental margin. Both regional facies relations and provenance indicate that the Jidula was most probably derived from basement rocks of the Indian continent, indicating that collision between India and Asia had not yet affected this region. Sandstone petrography of the younger Youxia and Shenkeza Formations shows a significant amount of immature framework grains, with compositions corresponding to the "recycled orogen" provenance field, consistent with the geochemistry of sandstone and shale samples and the occurrence of Cr-rich spinels with typical composition of spinels in fore-arc peridotites. The sharp change of the sedimentary compositions between the times of deposition of the Jidula and Youxia formations is the change from shelf to foredeep basin sedimentation and from Indian to Asian provenance. The persistence of carbonate shelf sedimentation to the base of the Youxia Formation shows that the onset of continental collision in the Zhepure Shan region of the eastern central Himalaya is dated as planktonic zone P-8 of the late Ypresian at 50.6 ± 0.2 Ma. This is exactly the same age reported by Garzanti et al. (1996) from Zanskar and implies the collision began synchronously along much of the Himalaya. Further, this new estimate implies that initiation of collision and the marked decrease in convergence rate between India and Asia are not synchronous but required approximately 3 m.yr. for collision to affect convergence rates.

REFERENCES CITED

Allan, J. F.; Sack, R. O.; and Batiza, R. 1988. Cr-rich spinels as petrogenetic indicators: MORB-type lavas from the Lamont seamount chain, eastern Pacific. Am. Mineral. 73:741–753.

Allen, P. A.; Burgess, P. M.; Galewsky, J.; and Sinclair, H. D. 2001. Flexural-eustatic numerical model for drowning of the Eocene perialpine carbonate ramp and implications for Alpine geodynamics. Geol. Soc. Am. Bull. 113:1052–1066.

Barnes, S. J., and Roeder, P. L. 2001. The range of spinel compositions in terrestrial mafic and ultramafic rocks. J. Petrol. 42:2279–2302.

Berggren, W. A.; Kent, D. V.; Swisher, C. C.; and Aubry, M. P. 1995. A revised Cenozoic geochronology and chronostratigraphy. *In* Berggren, W. A., and Kent, D. V., eds. Geochronology, time scales and global stratigraphic correlation. SEPM Spec. Publ. 54:129–212.

Bhatia, M. R. 1983. Plate tectonics and geochemical composition of sandstones. J. Geol. 91:611–627.

———. 1985. Composition and classification of Paleozoic flysch mudrocks of eastern Australia: implications in provenance and tectonic setting interpretation. Sediment. Geol. 41:249–268.

Bhatia, M. R., and Crook, K. 1986. Trace element characteristics of greywackes and tectonic setting discrimination of sedimentary basins. Contrib. Mineral. Petrol. 92:181–193.

Bock, B.; Mclennan, S. M.; and Hanson, G. N. 1998. Geochemistry and provenance of the middle Ordovician Austin Glen Member (Normanskill Formation) and the Taconian Orogeny in New England. Sedimentology 45:635–655.

Bossart, P., and Ottiger, R. 1989. Rocks of the Murree formation in the northern Pakistan, indicators of a descending foreland basin of late Paleocene to middle Eocene age. Eclogae Geol. Helv. 82:133–165.

Bryndzia, L. T., and Wood, B. J. 1990. Oxygen thermobarometry of abyssal spinel peridotites: the redox state and C-O-H volatile composition of the Earth's suboceanic upper mantle. Am. J. Sci. 290:1093–1116.

Burg, J., and Chen, G. 1984. Tectonics and structural formation of southern Tibet, China. Nature 311:219–223.

Clift, P. D.; Carter, A.; Krol, M.; and Kirby, E. 2002. Constraints on India-Eurasia collision in the Arabian Sea region taken from the Indus Group, Ladakh Himalaya, India. *In* Clift, P. D.; Kroon, D.; Gaedicke, C.; and Craig, J., eds. The tectonic and climatic evolution of the Arabian Sea region. Geol. Soc. Lond. Spec. Publ. 195:97–116.

Clingolani, C. A.; Manassero, M.; and Abre, P. 2003. Composition, provenance, and tectonic setting of Ordovician siliciclastic rocks in the San Rafael block: southern extension of the Precordillera crustal fragment, Argentina. J. S. Am. Earth Sci. 16:91–106.

Cookenboo, H. O.; Bustin, R. M.; and Wilks, K. R. 1997. Detrital chromian spinel compositions used to reconstruct the tectonic setting of provenance: implications for orogeny in the Canadian Cordillera. J. Sediment. Res. 67:116–123.

Critelli, S., and Garzanti, E. 1994. Provenance of the lower Tertiary Murree redbeds (Hazara-Kashmir Sytaxis, Pakistan) and initial rising of the Himalayas. Sediment. Geol. 89:265–284.

Cullers, R. L.; Basu, A.; and Suttner, L. J. 1988. Geochemical signature of provenance in sand-size material in soils and stream sediments near the Tobacco Root batholith, Montana, USA. Chem. Geol. 70:335–348.

DeCelles, P. G.; Gehrels, G. E.; Quade, L.; and Qjha, T. P. 1998. Eocene–early Miocene foreland basin development and the history of Himalayan thrusting, western and central Nepal. Tectonics 17:741–765.

de Sigoyer, J.; Chavagnac, V.; Blichert-Tift, J.; Villa, I.; Luais, B.; Guillot, S.; Cosca, M.; and Mascle, G. 2000. Dating the Indian continental subduction and collisional thickening in the northwest Himalaya: multichronology of the Tso Morari eclogites. Geology 28:487–490.

———. 2001. Dating the Indian continental subduction and collisional thickening in the northwest Himalaya: multichronology of the Tso Morari eclogites: comments and reply. Geology 29:192.

Dick, H. J. B., and Bullen, T. 1984. Chromian spinel as a petrogenetic indicator in abyssal and alpine-type peridotites and spatially associated lavas. Contrib. Mineral. Petrol. 86:54–76.

Dickinson, W. 1985. Interpreting provenance relations from detrital modes of sandstones. *In* Zuffa, G., ed. Provenance of arenites. NATO Advanced Study Institute Series 148, p. 333–361. Reidel, Dordrecht.

Dickinson, W., and Suczek, C. 1979. Plate tectonics and sandstones composition. Am. Assoc. Petrol. Geol. Bull. 63:2164–2172.

Durr, S. 1996. Provenance of Xigaze fore-arc basin clastic rocks (Cretaceous, South Tibet). Geol. Soc. Am. Bull. 108:669–684.

Einsele, G.; Liu, B.; Dürr, S.; Frisch, W.; Liu, G.; Luterbacher, H. P.; Ratschbacher, L.; et al. 1994. The Xigaze forearc basin, evolution and facies architecture (Cretaceous, Tibet). Sediment. Geol. 90:1–20.

Evans, M. J., and Mange-Rajetzky, M. A. 1991. The provenance of sediments in the Barreme thrust-top basin, Haute-Provenance, France. *In* Morton, A. C.; Todd, S. P.; and Haughton, P. D. W., eds. Developments in sedimentary provenance studies. Geol. Soc. Lond. Spec. Publ. 57:323–343.

Gansser, A. 1964. Geology of the Himalayas. London, Wiley, 284 p.

Ganssloser, M. 1999. Detrital chromian spinels in Rhenohercynian greywackes and sandstones (Givetain-

Visean, Variscides, Germany) as indicators of ultra-mafic source rocks. Geol. Mag. 136:437–451.

Garzanti, E. 1999. Stratigraphy and sedimentary history of the Nepal Tethys Himalayan passive margin. *In* Upreti, B. N., and Le Fort, P., eds. Advances on the geology of the Himalaya: focus on Nepal. J. Asian Earth Sci. 17:805–827.

Garzanti, E.; Baud, A.; and Mascle, G. 1987. Sedimentary record of the northward flight of India and its collision with Eurasia (Ladakh Himalayas, India). Geodinam. Acta 1:297–312.

Garzanti, E.; Critelli, S.; and Ingersoll, R. 1996. Paleo-geographic and paleotectonic evolution of the Himalayan Range as reflected by detrital modes of Tertiary sandstones and modern sands (Indus transect, India and Pakistan). Geol. Soc. Am. Bull. 108:631–642.

Guillot, S.; Garzanti, E.; Baratoux, D.; Marquer, D.; Maheo, G.; and de Sigoyer, J. 2003. Reconstructing the total shortening history of NW Himalaya. Geochem. Geophys. Geosyst. 4:1–22.

Hayashi, K.; Fujisawa, H.; Holland, H. D.; Ohmoto, H. 1997. Geochemistry of ~1.9 Ga sedimentary rocks from northeastern Labrador, Canada. Geochim. Cosmochim. Acta 61:4114–4137.

Hiscott, R. N. 1984. Ophiolitic source rocks for Taconic-age flysch: trace element evidence. Geol. Soc. Am. Bull. 95:1261–1267.

Holland, H. D. 1984. The chemical evolution of the atmosphere and oceans. Princeton University Press, Princeton, NJ.

Humphreys, B.; Morton, A. C.; Hallsworth, C. R.; Gatliff, R. W.; and Riding, J. B. 1991. An integrated approach to provenance studies: a case example from the Upper Jurassic of the Central Graben, North Sea. *In* Morton, A. C.; Todd, S. P.; and Haughton, P. D. W., eds. Developments in sedimentary provenance. Geol. Soc. Lond. Spec. Publ. 57:251–262.

Ingersoll, R. V.; Bullard, T. F.; Ford, R. L.; Grimm, J. P.; Pickle, J. D.; and Sares, S. W. 1984. The effect of grain size on detrital modes: a test of the Gazzi-Dickinson point-counting method. J. Sediment. Petrol. 49:103–116.

Irvine, T. N. 1967. Chromium spinel as a petrogenetic indicator. II. Petrologic applications. Can. J. Earth Sci. 4:71–103.

Jan, M. Q.; Khan, M. A.; and Windley, B. F. 1992. Exsolution in Al-Cr-Fe3+-rich spinels from the Chilas mafic-ultramafic complex, Pakistan. Am. Mineral. 77:1074–1079.

Jan, M. Q., and Windley, B. F. 1990. Chromian spinel-silicate chemistry in ultramafic rocks of the Jijal Complex, Northwest Pakistan. J. Petrol. 31:667–715.

Johnson, D. M.; Hooper, P. R.; and Conrey, R. M. 1999. XRF analysis of rocks and minerals for major and trace elements on a single low dilution Li-tetraborate fused bead. Adv. X-Ray Anal. 41:843–867.

Kamenetsky, V.; Crawforod, A. J.; and Meffre, S. 2001. Factors controlling chemistry of magmatic spinel: an empirical study of associated olivine, Cr-spinel and

melt inclusions from primitive rocks. J. Petrol. 41:655–671.

Kamperman, M.; Danyushevsky, L. V.; Taylor, W. R.; and Jablonski, W. 1996. Direct oxygen measurement of Cr-rich spinel: implication for spinel stoichiometry. Am. Mineral. 81:1186–1194.

Knaack, C.; Cornelius, S.; and Hooper, P. 1994. Trace element analyses of rocks and minerals by ICP-MS. Geoanalytical Library, Washington State University, Pullman. http://www.wsu.edu:8080/~geology/Pages/Services/ICP.html.

Lee, Y. 1999. Geotectonic significance of detrital chromian spinel: a review. Geosci. J. 3:23–29.

Lenaz, D.; Kamenetsky, V.; Crawford, A. J.; and Princivalle, F. 2000. Melt inclusions in detrital spinel from SE Alps (Italy-Slovenial): a new approach to provenance studies of sedimentary basins. Contrib. Mineral. Petrol. 139:748–758.

Le Pichon, X.; Fournier, M.; and Jolivet, L. 1992. Kinematics, topography, and extrusion in the India-Eurasia collision. Tectonics 11:1085–1098.

Mack, G. H.; James, W. C.; and Monger, H. C. 1993. Classification of paleosols. Geol. Soc. Am. Bull. 105:129–136.

Mange, M. A., and Maurer, H. F. W. 1992. Heavy minerals in color. Chapman & Hall, London, 147 p.

McLennan, S. M.; Hemming, S. R.; McDaniel, D. K.; and Hanson, G. N. 1993. Geochemical approaches to sedimentation, provenance, and tectonics. *In* Johnsson, M. J., and Base, A., eds. Processes controlling the composition of clastic sediments. Geol. Soc. Am. Spec. Pap. 284:21–40.

McLennan, S. M.; Taylor, S. R.; McCulloch, M. T.; and Maynard, J. B. 1990. Geochemical and Nd-Sr isotope composition of deep sea turbidites: crustal evolution and plate tectonic associations. Geochim. Cosmochim. Acta. 54:2015–2050.

Morton, A. C. 1985. Heavy minerals in provenance studies. *In* Zuffa, G. G., ed. Provenance of arenites. Reidel, Dordrecht, p. 249–277.

———. 1991. Geochemical studies of detrital heavy minerals and their application to provenance studies. *In* Morton, A. C.; Todd, S. P.; and Haughton, P. D. W., eds. Developments in sedimentary provenance studies. Geol. Soc. Lond. Spec. Publ. 57:31–45.

Najman, Y., and Garzanti, E. 2000. An integrated approach to provenance studies: reconstructing early Himalayan paleogeography and tectonic evolution from Tertiary foredeep sediments, N. India. Geol. Soc. Am. Bull. 112:435–449.

Najman, Y.; Pringle, M.; Godin, L.; and Oliver, G. 2001. New dating of the oldest Himalayan continental foreland basin sediments forces reconsideration of current models of India-Eurasia collision. Nature 410:194–197.

———. 2002. A reinterpretation of the Balakot Formation: implications for the tectonic evolution of the NW Himalaya, Pakistan. Tectonics 21:1–18.

Najman, Y. M. R.; Pringle, M. S.; Johnson, M. R. W.; Robertson, A. H. F.; and Wijbrans, J. R. 1997. Laser

40Ar/39Ar dating of single detrital muscovite grains from early foreland basin sediments in India: implications for early Himalayan evolution. Geology 25: 535–538.

Nesbitt, H. W., and Young, G. M. 1982. Early Proterozoic climates and plate motions inferred from major element chemistry of lutites. Nature 299:715–717.

Parkinson, I. J., and Pearce, J. A. 1998. Peridotites from the Izu-Bonin-Mariana Forearc (ODP Leg 125): evidence for mantle melting and melt-mantle interaction in a supra-subduction zone setting. J. Petrol. 39:1577–1618.

Patriat, P., and Achache, J. 1984. India-Eurasia collision chronology has implications for crustal shortening and driving mechanism of plates. Nature 311:615–621.

Pearce, J., and Deng, W. 1988. The ophiolites of the Tibetan Geotraverses, Lhasa to Golmud (1985) and Lhasa to Kathmandu (1986). Philos. Trans. R. Soc. Lond. A 327:215–238.

Pivnik, D. A., and Wells, N. A. 1996. The transition from Tethys to the Himalaya as recorded in northwest Pakistan. Geol. Soc. Am. Bull. 108:1295–1313.

Pober, E., and Faupl, P. 1988. The chemistry of detrital spinels and its application for the geodynamic evolution of the Eastern Alps. Geol. Rundsch. 77:641–670.

Qayyum, M.; Niem, A. R.; and Lawrence, R. D. 2001. Detrital modes and provenance of the Paleogene Khojak Formation in Pakistan: implications for early Himalayan orogeny and unroofing. Geol. Soc. Am. Bull. 113:320–332.

Rahman, M. J. J., and Faupl, P. 2003. The composition of the subsurface Neogene shales of the Surma group from the Sylhet Trough, Bengal Basin, Bangladesh. Sediment. Geol. 155:407–417.

Richter, F. R.; Rowley, D. B.; and DePaolo, D. J. 1992. Sr isotope evolution of seawater: the role of tectonics. Earth Planet. Sci. Lett. 109:11–23.

Roeder, P. L. 1994. Chromite: from the fiery rain of chondrules to the Kilauea Iki lava lake. Can. Mineral. 32: 729–746.

Rolland, Y.; Picard, C.; Pecher, A.; Lapierre, H.; Bosch, D.; and Keller, F. 2002. The Cretaceous Ladakh arc of NW Himalaya-slab melting and melt-mantle interaction during fast northward drift of Indian plate. Chem. Geol. 182:139–178.

Roser, B. P., and Korsch, R. J. 1986. Determination of tectonic setting of sandstone-mudstone suites using SiO$_2$ content and K$_2$O/Na$_2$O ratio. J. Geol. 94:635–650.

———. 1988. Provenance signatures of sandstone-mudstone suites determined using discrimination function analysis of major element data. Chem. Geol. 67:119–139.

Rowley, D. 1996. Age of initiation of collision between India and Asia: a review of stratigraphic data. Earth Planet. Sci. Lett. 145:1–13.

———. 1998. Minimum age of initiation of collision between India and Asia north of Everest based on the subsidence history of the Zhepure Mountain section. J. Geol. 106:229–235.

Rowley, D., and Kidd, W. S. F. 1981. Stratigraphic relationships and detrital composition of the medial Ordovician flysch of western New England: implications for the tectonic evolution of the Taconic Orogeny. J. Geol. 89:199–218.

Sciunnach, D., and Garzanti, E. 1996. Detrital chromian spinels record tectono-magmatic evolution from Carboniferous rifting to Permian spreading in Neotethys (India, Nepal and Tibet). Ofioliti 22:101–110.

Scowen, P. A. H.; Roeder, P. L.; and Helz, R. T. 1991. Reequilibration of chromite within Kilauea Iki lava lake, Hawaii. Contrib. Mineral. Petrol. 107:8–20.

Searle, M. 2001. Dating the Indian continental subduction and collisional thickening in the northwest Himalaya: multichronology of the Tso Morari eclogites: comments and reply. Geology 29:191.

Sengor, A.; Altiner, D.; Cin, A.; Ustaomer, T.; and Hsu, K. J. 1988. Original assembly of the Tethyside orogenic collage at the expense of Gondwanaland. *In* Audley-Charles, M. G., and Hallam, A., eds. Gondwana and tethys. Geol. Soc. Lond. Spec. Publ. 37:119–181.

Taylor, S. R., and McLennan, S. M. 1985. The continental crust: its composition and evolution. Blackwell, Oxford, 312 p.

Walker, R. G., ed. 1979. Facies models. Geosci. Can. Reprint Ser. 1, Geol. Assoc. Can. 211 p.

Wan, X.; Jansa, L. F.; and Sarti, M. 2002. Cretaceous and Paleogene boundary strata in southern Tibet and their implication for the India-Eurasia collision. Lethaia 36: 131–146.

Wang, C.; Li, X.; Hu, X.; and Jansa, L. F. 2002. Latest marine horizon north Qomolangma (Mt Everest): implications for closure of Tethys seaway and collision tectonics. Terra Nova 14:114–120.

Wang, C.; Liu, Z.; and Hebert, R. 2000. The Yarlung-Zangbo paleo-ophiolite, southern Tibet: implications for the dynamic evolution of the Yarlung-Zangbo Suture Zone. J. Asian Earth Sci. 18:651–661.

Willems, H., and Zhang, B. G. 1993. Cretaceous and lower Tertiary sediments of the Tethys Himalaya in the area Tingri (South Tibet, PR China). Ber. FB Geowiss. Univ. Bremen 38:29–47.

Willems, H.; Zhou, Z.; Zhang, B.; and Graefe, K. U. 1996. Stratigraphy of the Upper Cretaceous and Lower Tertiary strata in the Tethyan Himalayas of Tibet (Tingri area, China). Geol. Rundsch. 85:723–754.

Yin, A., and Harrison, M. 2000. Geologic evolution of the Himalayan-Tibetan orogen. Annu. Rev. Earth Planet. Sci. 28:211–280.

Young, G. M. 2002. Geochemical investigation of a Neoproterozoic glacial unit: the Mineral Fork Formation in the Wasatch Range, Utah. Geol. Soc. Am. Bull. 114: 387–399.

Young, G. M.; Brunn, V.; Gold, D. J. C.; and Minter, W. E. L. 1998. Earth's oldest reported glaciation: physical and chemical evidence from the Archean Mozaan Group (~2.9 Ga) of South Africa. J. Geol. 106:523–538.

Zhang, B., and Geng, L. 1983. A further knowledge of the Early Tertiary strata in southern Xizang. J. Stratr. 7: 25–30.

Zhou, M.; Robinson, P. T.; Malpas, J.; and Li, Z. 1996. Podiform chromitites from the Luobusa ophiolites (southern Tibet): implications for melt rock interaction and chromite segregation. J. Petrol. 37:3–21.

Zhu, B.; Kidd, W. S. F.; Rowley, D.; and Currie, B. 2004. Chemical compositions and tectonic significance of chrome-rich spinels in Tianba Flysch, southern Tibet. J. Geol. 112:417–434.

Zuffa, G. 1980. Optical analysis of arenites: their composition and classification. J. Sediment. Petrol. 50:21–29.